NANO · MICRO small

www.small-journal.com

Spatial Micropatterning of Growth Factors in 3D Hydrogels for Location-Specific Regulation of Cellular Behaviors

*Oju Jeon, Keewon Lee, and Eben Alsberg**

Growth factors are potent stimuli for regulating cell function in tissue engineering strategies, but spatially patterning their presentation in 3D in a facile manner using a single material is challenging. Micropatterning is an attractive tool to modulate the cellular microenvironment with various biochemical and physical cues and study their effects on stem cell behaviors. Implementing heparin's ability to immobilize growth factors, dual-crosslinkable alginate hydrogels are micropatterned in 3D with photocrosslinkable heparin substrates with various geometries and micropattern sizes, and their capability to establish 3D micropatterns of growth factors within the hydrogels is confirmed. This 3D micropatterning method could be applied to various heparin binding growth factors, such as fibroblast growth factor-2, vascular endothelial growth factor, transforming growth factor-betas and bone morphogenetic proteins while retaining the hydrogel's natural degradability and cytocompability. Stem cells encapsulated within these micropatterned hydrogels have exhibited spatially localized growth and differentiation responses corresponding to various growth factor patterns, demonstrating the versatility of the approach in controlling stem cell behavior for tissue engineering and regenerative medicine applications.

Tissue engineering aims to develop biologically functional substitutes for the purpose of restoring and/or replacing damaged, injured, or lost native tissues.[1] One strategy is to incorporate cells within a biomaterial that provides a 3D microenvironment capable of regulating cell function and ultimately driving new tissue formation.[2] During development and healing processes, cells continuously sense and respond to a variety of biochemical and physical signals from their extracellular microenvironment that play a central role in influencing their behavior, such as migration, growth, survival, apoptosis, and differentiation.[3] The temporal and spatial presentation of these signals is critical for the formation of tissues with complex composition and morphology.[4] Thus, the ability to engineer biomaterial systems capable of partially recapitulating the finely orchestrated presentation of these signals both in time and space may permit the mimicking of how these tissues are formed naturally.

Recent progress in micropatterning in biomaterial scaffolds has enabled manipulation of the 3D environment up to the micrometer scale and provided insights in stem cell behavior. For example, a previous study has shown that micropatterning hyaluronic acid hydrogels with degradable peptide-crosslinked regions permitted control over the location of mesenchymal stem cell (MSC) spreading,[5] illustrating its usefulness for regulating stem cell remodeling. In addition, our group has reported that changes in the size of micropatterned regions of a dual-crosslinked alginate hydrogel system with different physical properties had a significant influence on stem cell proliferation and osteogenic and chondrogenic differentiation.[6] Further developments to fabricate micropatterned hydrogels with tailorable physical cues are underway; however, few studies have attempted to construct spatial 3D patterns of growth factors, which are bioactive molecules that are known to play a critical role in the development of tissues. To date, strategies to engineer 3D micropatterns of growth factors in hydrogels employ sophisticated fabrication procedures that require expertise and expensive equipment and materials, cannot be used to fabricate clinically relevant macroscale 3D constructs, and/or do not permit simultaneous encapsulation of cells.[7]

Over the past decade, heparin functionalization has emerged as an attractive method to control the delivery of heparin-binding growth factors to cells.[8] Heparin is a highly negatively charged polysaccharide, naturally found in the extracellular matrix (ECM), and is also known to sequester various growth factors and ECM proteins.[8,9] Recently, our laboratory described a new bioactive hydrogel system formed by photocrosslinking of methacrylated heparin and methacrylated alginate, resulting in the covalent coupling of the heparin to the resulting hydrogel backbone.[10] The heparin-photofunctionalized alginate hydrogels permitted the controlled and sustained release of multiple growth factors that have an affinity with heparin, such as fibroblast growth factor-2 (FGF-2), vascular endothelial growth factor (VEGF), transforming growth factor-beta 1

Prof. O. Jeon, K. Lee, Prof. E. Alsberg
Department of Biomedical Engineering
Case Western Reserve University
Cleveland, OH 44106, USA
E-mail: eben.alsberg@case.edu
Prof. E. Alsberg
Department of Orthopaedic Surgery
Case Western Reserve University
Cleveland, OH 44106, USA

DOI: 10.1002/smll.201800579

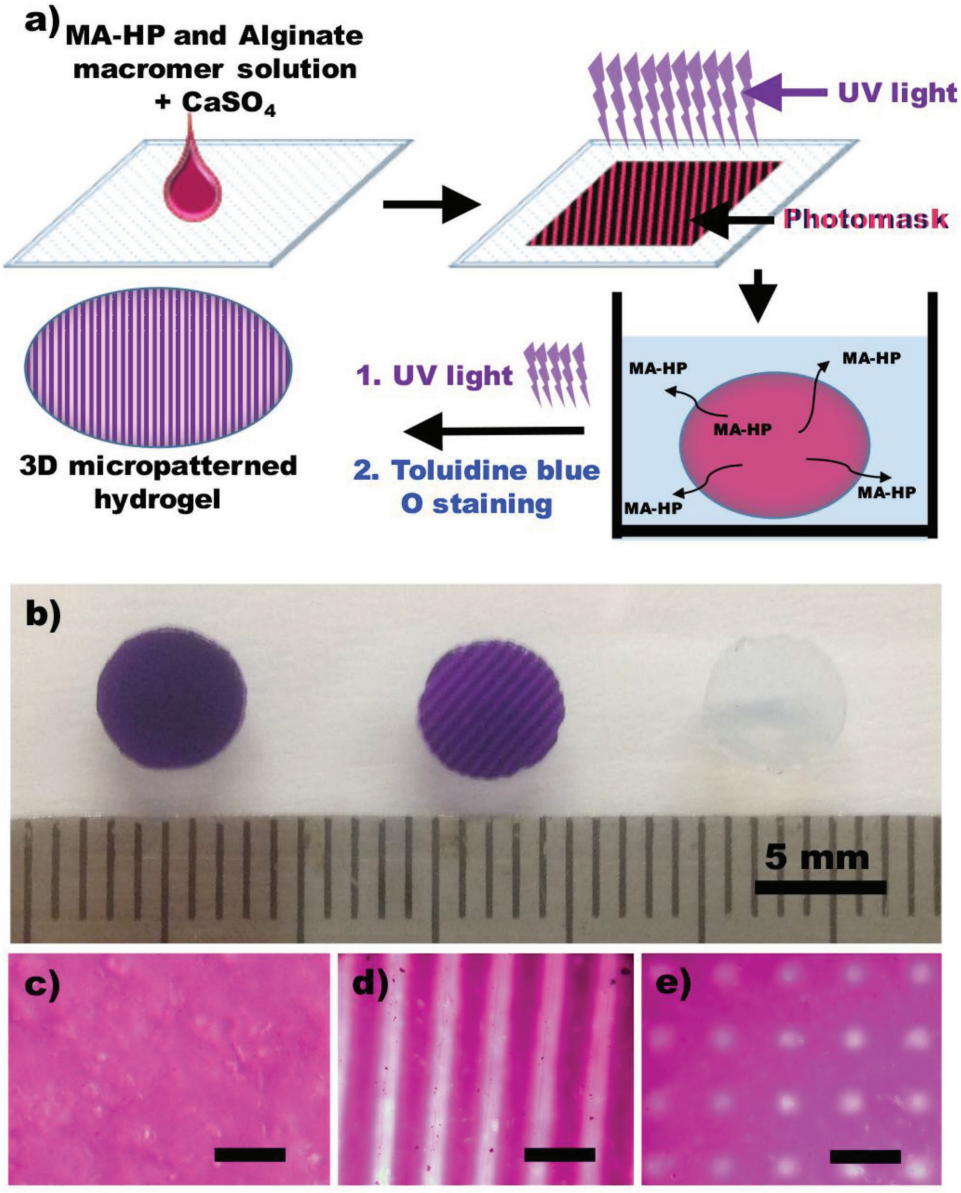

Figure 1. Fabrication of a heparin micropatterned dual-crosslinked alginate hydrogel. a) Schematic illustration of the preparation of a heparin micropatterned dual-crosslinked alginate hydrogel. b) Photograph of a dual-crosslinked heparin/alginate hydrogel without a micropattern (left), a striped-micropatterned (250 µm) dual-crosslinked heparin/alginate hydrogel, and a dual-crosslinked alginate hydrogel without heparin. Photomicroscopic images of a toluidine blue O stained c) dual-crosslinked heparin/alginate hydrogel without a micropattern, d) stripe-micropatterned (250 µm) hydrogel, and e) grid-micropatterned (200 µm) dual-crosslinked heparin/alginate hydrogel.

and bone morphogenetic protein-2 (BMP-2), and regulation of encapsulated stem cell behaviors.[10] Photolithographic techniques, such as the use of a photomask, permit the formation of bulk hydrogels of various geometries and dimensions with heparin-based growth factor sequestering capacity, as demonstrated with heparin-thiolates and poly(ethylene glycol)-diacrylates.[11] However, this approach has only been shown to allow for the formation of gels with spatially uniform growth factor sequestration. There are no reports to date of 3D micropatterning of locally defined regions of growth factor sequestration within hydrogels and subsequent spatial control over encapsulated cell responses as a result of these biochemical cues.

The purpose of this study was to develop a simple, cheap, and cytocompatible but robust 3D growth factor-micropatterned hydrogel system by photofunctionalization of methacrylated heparin into dual-crosslinkable alginate hydrogels, and use it to evaluate the effect of micropatterned growth factors on encapsulated stem cell behavior. Alginate was oxidized and methacrylated (Figure S1, Supporting Information) to form biodegradable, dual-crosslinkable hydrogels by ionic crosslinking with calcium ions (Ca^{2+}) and photocrosslinking under ultraviolet (UV) light (**Figure 1**a). To incorporate and micropattern the heparin into the dual-crosslinkable alginate hydrogels during the photopolymerization process, methacrylate groups were

covalently coupled to the heparin backbone by reacting the carboxylic acid groups of the heparin with the amine groups of 2-aminoethyl methacrylates using standard carbodiimide chemistry (Figure S2, Supporting Information). The overall strategy for the formation of 3D heparin-micropatterned hydrogels is depicted in Figure 1a.

First, uniform ionic crosslink networks were formed between the alginate macromers and Ca^{2+}. Then, the second crosslink networks were formed by photopolymerization of the methacrylate groups of the alginate and heparin in the ionically crosslinked heparin-containing alginate hydrogels through photomasks, which created micropatterns of photocrosslinked regions. Unreacted methacrylated heparin was removed from the single-crosslinked regions of the micropatterned dual-crosslinked hydrogel by incubating in media. To minimize any potential mechanical property differences between the single- and dual-crosslinked regions on encapsulated cell behavior, micropatterned dual-crosslinked hydrogels were then further photocrosslinked under UV light without a photomask to crosslink the methacrylate groups of alginate in the originally single-crosslinked regions (Figure 3, Supporting Information). To visualize the heparin micropatterns in the hydrogel disks, 3D heparin-micropatterned, dual-crosslinked hydrogels were stained with toluidine blue O. A dual-crosslinked hydrogel containing methacrylated heparin formed without the use of a photomask (Figure 1b, left and Figure 1c) was stained entirely by toluidine blue O, indicating that heparin was coupled uniformly to the hydrogel. In contrast, toluidine blue O was not observed in a dual-crosslinked hydrogel formed without heparin (Figure 1b, right). Importantly, when a photomask with 250 μm wide stripes was used, stripe patterns were visually confirmed in the 3D heparin-micropatterned, dual-crosslinked alginate hydrogel (Figure 1b, middle and Figure 1d). To illustrate the versatility of this micropatterning approach, grid-shaped micropatterns (200 μm) were also fabricated (Figure 1e). Since this simple but robust method provides precise control over 3D heparin micropatterns, this system could be a useful platform to investigate the effects of micropatterned growth factors that have a binding affinity with heparin on the behaviors of stem cells, such as adipose tissue-derived stem cells, MSCs, induced pluripotent stem cells, and embryonic stem cells.

To demonstrate that micropatterned heparin in dual-crosslinked alginate hydrogels could create 3D growth factor micropatterns, VEGF was incorporated into the constructs and detected via immunostaining to verify successful micropatterning. VEGF (red) could be 3D micropatterned in the hydrogels with various dimensions and geometries as shown in **Figure 2**. Since VEGF induces neovascularization

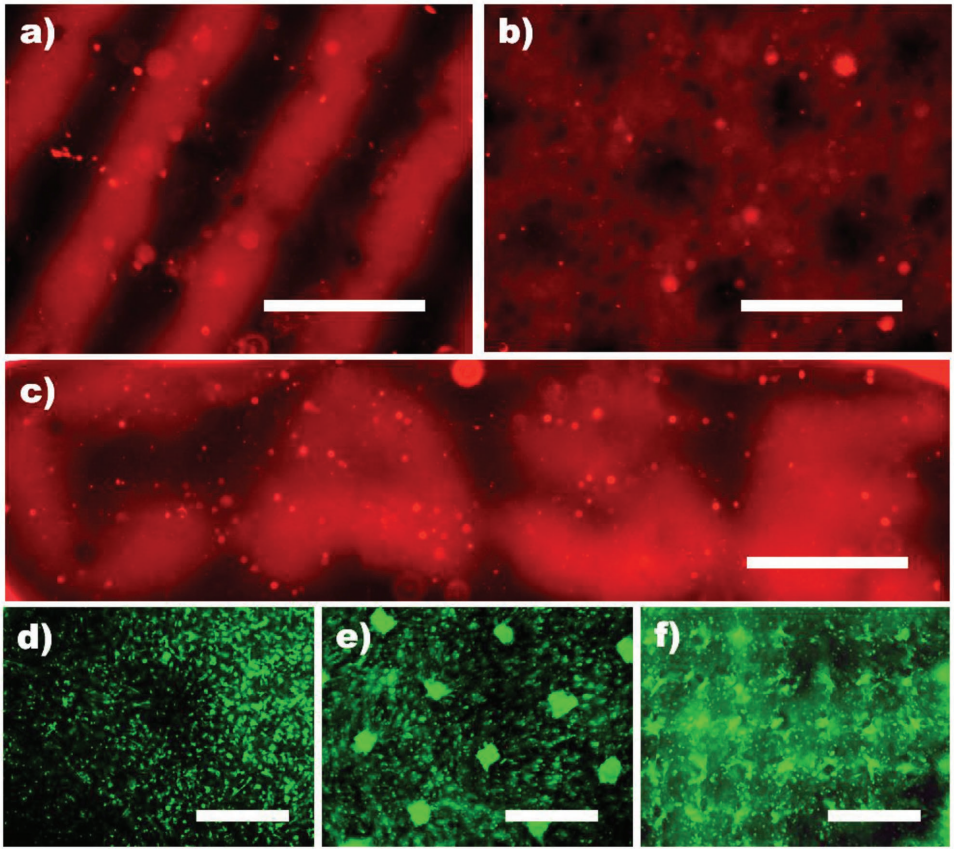

Figure 2. Formation of growth factor micropatterned dual-crosslinked alginate hydrogels and local promotion of hMSC clustering. Fluorescence photomicroscopic images of a) stripe (250 μm), b) grid (200 μm), and c) letters (250 μm, case) of VEGF micropatterned, dual-crosslinked alginate hydrogels stained with VEGF antibody. Representative live (fluorescein diacetate, green)/dead (ethidium bromide, red) photomicroscopic images of hMSCs encapsulated in d) grid (200 μm) micropatterned dual-crosslinked heparin/alginate hydrogels without FGF-2 and e) square (50 μm × 50 μm), and f) checkerboard (100 μm) micropatterned FGF-2 in dual-crosslinked heparin/alginate hydrogels after 28 d culture in vitro. All scale bars indicate 250 μm.

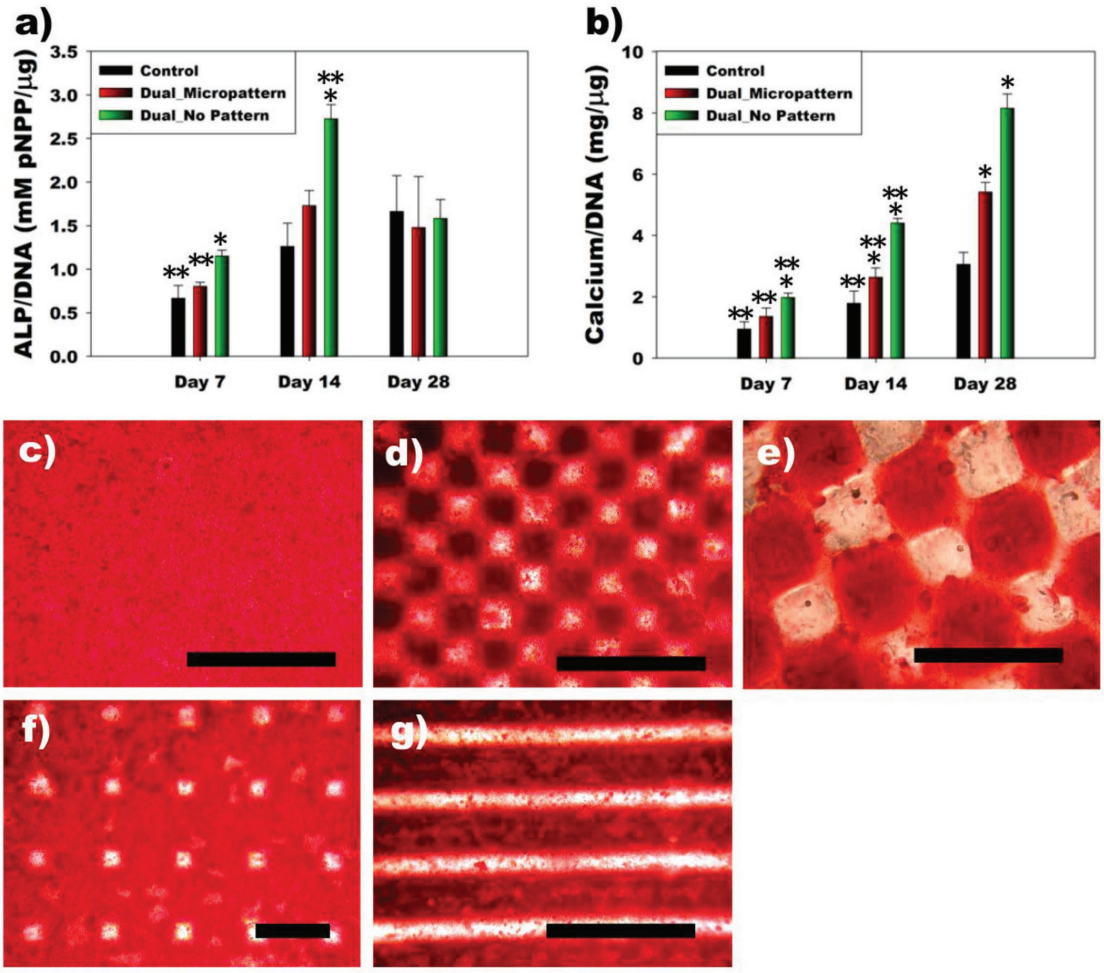

Figure 3. Encapsulation of hMSCs in BMP-2 micropatterned dual-crosslinked alginate hydrogels induces micropatterned hMSC osteogenesis. Quantification of a) ALP/DNA and b) calcium/DNA produced by hMSCs encapsulated within a dual-crosslinked heparin/alginate hydrogel without BMP-2 (control), a checkerboard micropattern (200 μm) of BMP-2 in a dual-crosslinked heparin/alginate hydrogel (Dual_Micropattern), and a BMP-2-loaded dual-crosslinked heparin/alginate hydrogel without a micropattern (Dual_No Pattern). $*p < 0.05$ compared to other groups at a specific time point. $**p < 0.05$ compared to other time points within a specific group. Optical photomicroscopic images of mineralization of hMSCs encapsulated in c) Dual_No Pattern and micropatterned d,e) checkerboards (100 and 200 μm), f) a grid (200 μm) and g) stripes (250 μm) of BMP-2 micropatterned hydrogels after 28 d culture in osteogenic differentiation media. All scale bars indicate 400 μm.

and angiogenesis as well as supports cell survival and differentiation,[12] this heparin-micropatterned dual-crosslinked alginate hydrogel system can provide a useful platform to regulate capillary morphogenesis and promote spatially regulated blood vessel formation in various tissue engineering applications.

While 3D micropatterned material presentation of cell adhesion ligands,[13] mechanical properties[6,14] and topographical features[15] have been shown to have the capacity to spatially control cell behavior, the capacity to regulate encapsulated cell function by growth factor micropatterning within biomaterials has not yet been demonstrated. To evaluate whether micropatterned growth factors in this system remained bioactive and could modulate cell behavior with spatial fidelity, human MSCs (hMSCs) were photoencapsulated within 3D FGF-2 micropatterned, dual-crosslinked alginate hydrogels. FGF-2 is a mitogen for hMSCs.[16] Cellular morphology of hMSCs varied between the FGF-2 immobilized and the nonimmobilized regions. hMSCs photoencapsulated in the FGF-2 immobilized regions grew into cell clusters, while hMSCs encapsulated in the FGF-2 nonimmobilized regions remained predominantly isolated through 28 d (Figure 2d,e). 3D clustering of cells better mimics development and healing of some tissues, such as bone,[17] cartilage,[18] and vasculature,[19] and cannot be replicated in conventional 2D culture. In this study, micropatterned FGF-2 in the dual-crosslinked heparin/alginate hydrogels yielded relatively uniform hMSC clusters within 3D hydrogels, which scaled in size with micropattern dimensions with high cell viability throughout both micropatterns (Figure 2d,e). This is a straightforward strategy for inducing the formation of development of mimetic cellular clusters of defined geometries in specific spatial locations within 3D hydrogels via local patterning of growth factor.

To investigate the effect of micropatterned growth factor on encapsulated stem cell differentiation, hMSCs seeded within 3D BMP-2 micropatterned, dual-crosslinked heparin/alginate hydrogels were cultured in osteogenic differentiation media for

28 d. BMP-2 is a strong osteoinductive cytokine. When the proliferation of encapsulated hMSCs in the hydrogels was examined by DNA content as a function of culture time, the DNA content significantly increased over 14 d (Figure S4a, Supporting Information). There was no significant difference in DNA content among any of the groups. hMSC/hydrogel constructs were evaluated for hMSC osteogenic differentiation by measuring alkaline phosphatase (ALP) activity, an early osteogenic differentiation marker. The ALP activity of encapsulated hMSCs normalized to DNA in the dual-crosslinked BMP-2 incorporated group without a micropattern was significantly higher at early time points (days 7 and 14) compared to the other groups; however, there were no significant differences between groups at the later time point (day 28, **Figure 3**a). In addition, total ALP content significantly increased in all groups up to day 14, and, importantly, was greatest in the Dual_No Pattern group, followed by the Dual_Micropattern group (Figure 4b, Supporting Information). Since the critical late-stage marker of osteogenic differentiation is mineralization, calcium deposition was then quantified. Calcium deposition of all groups significantly increased up to 28 d (Figure 3b and Figure S4c, Supporting Information). Calcium content normalized to DNA and total calcium content of the BMP-2-laden groups (Dual_Micropattern and Dual_No Pattern) were significantly higher than that of control at days 14 and 28. Dual_No Pattern group exhibited the highest calcium content at all time points. As shown in Figure 1b (left), heparin was immobilized throughout a dual-crosslinked hydrogel without micropatterning (Dual_No Pattern). Therefore, it is likely that more BMP-2 was immobilized in Dual_No Pattern group compared to Dual_Micropattern group. Retention of BMP-2 in dual-crosslinked heparin/alginate hydrogels accelerated both early (ALP) and late (calcium) osteogenic differentiation, and the increased rate and extent of differentiation was even more pronounced for the Dual_No Pattern group because more BMP-2 is retained compared to Control and Dual_Micropattern groups.

As discussed earlier, this technique provides precise control over 3D growth factor micropatterning. To demonstrate the capacity to spatially localize hMSC mineralization, hMSCs were encapsulated and osteogenically differentiated within various sizes and shapes of BMP-2 micropatterned within dual-crosslinked heparin/alginate hydrogels. While Dual_No Pattern group exhibited intense mineralization throughout whole hydrogel (Figure 3c), as shown in Figure 3d–g, BMP-2 micropatterns dictated the spatial location of hMSC mineralization.

Spatiotemporal control over the presentation of bioactive factors within biomaterials may be critical for partially recapitulating multifaceted and intricate developmental and regenerative processes to drive the engineering of complex tissues. Although there has been a great deal of interest in micropatterning of bioactive molecules within 3D biomaterials, to the best of our knowledge, this is the first report of a system capable of presenting 3D patterned growth factors within a biomaterial to encapsulated stem cells, and eliciting location-specific control over cellular function, such as clustering and differentiation.

In this study, we have engineered 3D growth factor-micropatterned hydrogels with various geometries and micropattern sizes by utilizing heparin's ability to immobilize growth factors. hMSCs encapsulated within growth factor-micropatterned hydrogels exhibited spatially localized growth and osteogenic differentiation responses corresponding to specific growth factor patterns. This system offers great potential for investigating the role of micropatterned growth factors on cell behavior and spatially controlling the formation of complex tissues.

Experimental Section

Bone marrow aspirates were obtained from the posterior iliac crest of healthy donors after informed signed consent under a protocol approved by the University Hospitals of Cleveland Institutional Review Board. Complete detailed methodology can be found in the Supporting Information.

Supporting Information

Supporting Information is available from the Wiley Online Library or from the author.

Acknowledgements

The authors gratefully acknowledge funding from the National Institutes of Health's National Institute of Arthritis and Musculoskeletal and Skin Diseases under award numbers R01AR069564 (EA) and R01AR066193 (EA). The contents of this publication are solely the responsibility of the authors and do not necessarily represent the official views of the National Institutes of Health.

Conflict of Interest

The authors declare no conflict of interest.

Keywords

alginate, drug delivery, growth factor micropatterns, stem cells, tissue engineering

Received: February 9, 2018
Revised: March 29, 2018
Published online:

[1] R. M. Nerem, *Tissue Eng.* **2006**, *12*, 1143.
[2] a) Y. Aizawa, S. C. Owen, M. S. Shoichet, *Prog. Polym. Sci.* **2012**, *37*, 645; b) A. Lober, A. Verch, B. Schlemmer, S. Hofer, B. Frerich, M. R. Buchmeiser, *Angew. Chem., Int. Ed.* **2008**, *47*, 9138.
[3] a) Y. Hu, J. O. You, J. Aizenberg, *ACS Appl. Mater. Interfaces* **2016**, *8*, 21939; b) R. O. Hynes, *Science* **2009**, *326*, 1216.
[4] M. P. Lutolf, J. A. Hubbell, *Nat. Biotechnol.* **2005**, *23*, 47.
[5] S. Khetan, J. A. Burdick, *Biomaterials* **2010**, *31*, 8228.
[6] O. Jeon, E. Alsberg, *Adv. Funct. Mater.* **2013**, *23*, 4765.
[7] a) R. G. Wylie, S. Ahsan, Y. Aizawa, K. L. Maxwell, C. M. Morshead, M. S. Shoichet, *Nat. Mater.* **2011**, *10*, 799; b) M. B. Applegate, J. Coburn, B. P. Partlow, J. E. Moreau, J. P. Mondia, B. Marelli, D. L. Kaplan, F. G. Omenetto, *Proc. Natl. Acad. Sci. USA* **2015**, *112*,

12052; c) H. H. Oh, H. Lu, N. Kawazoe, G. Chen, *Biotechnol. Prog.* **2012**, *28*, 773.
[8] C. McGann, K. Kiick, *Heparin-Functionalized Materials in Tissue Engineering Applications in Engineering Biomaterials for Regenerative Medicine*, Springer, New York, NY **2012**, pp. 225–250.
[9] W. H. Yu, S. Yu, Q. Meng, K. Brew, J. F. Woessner Jr., *J. Biol. Chem.* **2000**, *275*, 31226.
[10] O. Jeon, C. Powell, L. D. Solorio, M. D. Krebs, E. Alsberg, *J. Controlled Release* **2011**, *154*, 258.
[11] S. S. Shah, M. Kim, K. Cahill-Thompson, G. Tae, A. Revzin, *Soft Matter* **2011**, *7*, 3133.
[12] a) S. Masoumi Moghaddam, A. Amini, D. L. Morris, M. H. Pourgholami, *Cancer Metastasis Rev.* **2012**, *31*, 143; b) H. P. Gerber, A. K. Malik, G. P. Solar, D. Sherman, X. H. Liang, G. Meng, K. Hong, J. C. Marsters, N. Ferrara, *Nature* **2002**, *417*, 954.
[13] a) C. A. DeForest, K. S. Anseth, *Angew. Chem., Int. Ed.* **2012**, *51*, 1816; b) S. H. Lee, J. J. Moon, J. L. West, *Biomaterials* **2008**, *29*, 2962; c) C. A. DeForest, D. A. Tirrell, *Nat. Mater.* **2015**, *14*, 523.
[14] J. W. Nichol, S. T. Koshy, H. Bae, C. M. Hwang, S. Yamanlar, A. Khademhosseini, *Biomaterials* **2010**, *31*, 5536.
[15] a) A. Mata, L. Hsu, R. Capito, C. Aparicio, K. Henrikson, S. I. Stupp, *Soft Matter* **2009**, *5*, 1228; b) J. Kim, J. R. Staunton, K. Tanner, *Adv. Mater.* **2016**, *28*, 132.
[16] J. J. Auletta, E. A. Zale, J. F. Welter, L. A. Solchaga, *Stem Cells Int.* **2011**, *2011*, 1.
[17] M. Frohlich, W. L. Grayson, L. Q. Wan, D. Marolt, M. Drobnic, G. Vunjak-Novakovic, *Curr. Stem Cell Res. Ther.* **2008**, *3*, 254.
[18] C. Tacchetti, S. Tavella, B. Dozin, R. Quarto, G. Robino, R. Cancedda, *Exp. Cell Res.* **1992**, *200*, 26.
[19] J. Jabalee, T. A. Franz-Odendaal, *Dev. Biol.* **2015**, *406*, 52.